Research Square

Preprints are preliminary reports that have not undergone peer review.
They should not be considered conclusive, used to inform clinical practice,
or referenced by the media as validated information.

SOD2 rs4880 polymorphism predicts aggressive thyroid cancer: clinical validation of mitochondrial targeting sequence variation and re-evaluating in silico prediction limitations

Elisângela Souza Teixeira[1]
Universidade Estadual de Campinas (UNICAMP)
Marina Viana Alves[1]
Universidade Estadual de Campinas (UNICAMP)
Jacqueline Fátima Martins Almeida[1]
Universidade Estadual de Campinas (UNICAMP)
Matheus Nascimento[1]
Universidade Estadual de Campinas (UNICAMP)
Larissa Teodoro Rabi[1]
Universidade Estadual de Campinas (UNICAMP)
Karina Colombera Peres
Universidade Estadual de Campinas (UNICAMP)
Natássia Elena Bufalo
Universidade Estadual de Campinas (UNICAMP)
Laura Sterian Ward
ward@unicamp.br

Universidade Estadual de Campinas (UNICAMP)

Research Article

Keywords: Manganese superoxide dismutase, SOD2 rs4880, oxidative stress, thyroid

Posted Date: November 26th, 2026

DOI: https://doi.org/10.21203/rs.3.rs-11635019/v1

License: This work is licensed under a Creative Commons Attribution 4.0 International License. Read Full License

Additional Declarations: No competing interests reported.

Abstract

Manganese superoxide dismutase (MnSOD), encoded by SOD2, is a key mitochondrial antioxidant defense. We integrated in silico screening with clinical validation of SOD2 variants in thyroid cancer. Genotyping of rs4880 (Val16Ala), located within the precursor mitochondrial targeting sequence (MTS), was performed in 557 individuals (271 patients with thyroid nodules, 286 controls). Four rare nsSNPs were predicted to be deleterious in silico but had minor allele frequencies < 0.5%, precluding further analysis. Structure-based algorithms failed to predict the functional impact of the common rs4880 variant because it resides in the cleaved MTS rather than the mature catalytic domain. Rs4880 was not associated with cancer susceptibility (p = 0.396). However, the GG genotype was significantly more prevalent in malignant nodules (38.9%) than in benign nodules (12.7%; p = 0.031; G allele OR = 2.21, 95% CI: 1.43–3.42). Diagnostic ROC analysis for the GG genotype in discriminating malignant from benign nodules yielded 87.3% specificity, 92.3% positive predictive value, 38.9% sensitivity, and AUC = 0.631 (p = 0.0012). In multivariate models adjusted for age, sex, and histological subtype (papillary vs. follicular), the GG genotype independently predicted malignancy (OR = 3.82, p = 0.0031), capsular invasion (OR = 2.88, p = 0.0034), vascular invasion (OR = 3.65, p = 0.0241), and multifocality (OR = 3.12, p = 0.0007). Subgroup analysis restricted to papillary thyroid carcinoma (N = 164) confirmed independent associations with capsular invasion (OR = 3.15, p = 0.0020), vascular invasion (OR = 3.80, p = 0.0320), and multifocality (OR = 3.28, p = 0.0008). These findings suggest that the SOD2 rs4880 GG genotype may serve as a highly specific complementary biomarker and a potential modifier of thyroid tumor aggressiveness, warranting further validation.

1. INTRODUCTION

The thyroid gland relies on hydrogen peroxide (H_2O_2) as an essential cofactor for thyroid peroxidase (TPO)-mediated iodination of thyroglobulin. When H_2O_2 production exceeds antioxidant capacity, oxidative damage to DNA and other cellular components can contribute to mutagenesis and carcinogenesis [1]. This vulnerability is particularly relevant because reactive oxygen species (ROS) are generated constitutively during thyroid hormone synthesis, and their accumulation may become detrimental when redox balance is compromised [2,3].

ROS accumulation is a consistent feature of thyroid malignancies. Elevated ROS levels have been documented in papillary thyroid carcinoma (PTC) and correlate with tumor aggressiveness [2–4]. Patients with thyroid cancer also show systemic redox alterations, including increased serum ROS levels and reduced activity of superoxide dismutase and glutathione peroxidase [5,6]. These observations suggest that compromised antioxidant capacity may contribute to genomic instability and disease progression [7], although the underlying mechanisms remain incompletely defined.

Manganese superoxide dismutase (MnSOD), encoded by *SOD2* (6q25.3), catalyzes the dismutation of superoxide radicals in the mitochondrial matrix and is essential for maintaining mitochondrial redox homeostasis. Non-synonymous single nucleotide polymorphisms (nsSNPs) in *SOD2* can alter enzyme structure, stability, or activity [8,9] and have been associated with cancer susceptibility and progression in various malignancies [10–19]. However, the direction and magnitude of these associations vary across populations and tumor contexts, thereby limiting their clinical translation.

The role of *SOD2* polymorphisms in thyroid cancer remains poorly defined. Previous studies have reported inconsistent associations between *SOD2* variants and thyroid neoplasms, possibly reflecting differences in population genetics, allele frequencies, sample sizes, histological heterogeneity, and clinicopathological characteristics [20–22]. These discrepancies underscore the need to evaluate common *SOD2* variants in well-characterized cohorts with detailed clinicopathological annotation, rather than focusing exclusively on overall cancer susceptibility.

Because comprehensive experimental characterization of all *SOD2* nsSNPs is constrained by cost and scalability and requires adequate sample sizes [23,24], we first applied in silico prediction tools to prioritize variants with potentially functional consequences [25]. This screening identified four rare variants predicted to be deleterious; however, their minor allele frequencies (MAF < 0.5%) precluded clinical validation in our cohort. We therefore focused on the common rs4880 (Val16Ala) polymorphism.

Unlike most catalytic domain mutations, rs4880 resides within the precursor mitochondrial targeting sequence (MTS) [26,27]. Because standard structure-based algorithms evaluate mature protein crystal structures, they typically classify rs4880 as “neutral” and may misclassify signal-peptide variants [28]. However, experimental evidence suggests that signal peptide variations can alter mitochondrial precursor import efficiency and redox availability [29,30]. Furthermore, thyroid carcinomas encompass distinct histological entities, predominantly papillary (PTC) and follicular (FTC) carcinomas, with divergent molecular landscapes and invasive behaviors, as also illustrated by distinct antioxidant profiles in Hürthle cell neoplasms [20,22]. Evaluating rs4880 therefore requires subtype-adjusted multivariate modeling to avoid potential histological confounding.

We hypothesized that common *SOD2* variation in the MTS region alters tumor aggressiveness in a subtype-dependent manner. To test this hypothesis, we integrated in silico variant screening with clinical and molecular analysis of rs4880 in 271 patients with thyroid nodules and 286 healthy controls, evaluating its association with cancer susceptibility, the distinction between malignant and benign nodules, and clinicopathological features of tumor aggressiveness using multivariate models adjusted for age, sex, and histological subtype, alongside a dedicated PTC subgroup analysis.

2. MATERIALS AND METHODS

2.1 In Silico Analysis

2.1.1 Database Retrieval and Variant Selection

The dbSNP database (https://www.ncbi.nlm.nih.gov/snp/) was queried in February 2025 using the keyword "*SOD2*." The wild-type SOD2 protein sequence (UniProt ID: P04179) was retrieved from UniProtKB. A total of 44,861 variants were identified, of which 919 were annotated as missense (non-synonymous)

variants (2.05%). These 919 nsSNPs were selected for functional prediction using a sequential filtering strategy.

2.1.2 Functional Impact Prediction

The functional impact of the 919 nsSNPs was assessed using four sequence-based prediction tools: SIFT (score ≤ 0.05 considered deleterious) [31,32], PolyPhen-2 HumVar model (scores 0.95–1.00 considered probably damaging) [33,34], SNAP2 (score > 50 and reliability index ≥ 5 considered pathogenic) [35], and PANTHER (PSEP score ≥ 0.5 considered deleterious) [36,37]. Variants were prioritized if classified as deleterious by SIFT and probably damaging by PolyPhen-2. The 12 variants meeting these criteria were further evaluated.

2.1.3 Pathogenicity and Protein Stability

Pathogenic potential was evaluated using SNPs&GO [38], PMut [39], and PhD-SNP [40]. Protein stability changes were predicted using MutPred2 (*p* < 0.05) [41], I-Mutant 2.0 (ΔΔG < 0 kcal/mol indicating destabilization) [42], MUpro [43], and DynaMut2 using the MnSOD crystal structure (PDB ID: 8SKS) [44]; SDM was used as an additional stability/malfunction predictor [45].

2.1.4 Evolutionary Conservation and Structural Analysis

Evolutionary conservation was analyzed using ConSurf (scale 1–9) based on PDB ID: 8SKS [46,47]. Structural consequences were evaluated using the HOPE server [48]. MetaRNN ensemble pathogenicity scores were recorded. Protein-protein interaction networks and pathway enrichments were generated using STRING v12.0 [49] and Reactome 2024 [50,51].

2.1.5 Selection of SOD2 rs4880 for Clinical Investigation

Because variants with minor allele frequencies (MAF) below 0.5% could not be validated in the clinical cohort [52], clinical investigation was directed to common *SOD2* variants. Rs4880 (Val16Ala) was selected a priori based on: (i) MAF ≥ 0.5%; (ii) localization within the mitochondrial targeting sequence (MTS), a functional signal region not modeled by mature protein structure algorithms; and (iii) biological plausibility in modulating mitochondrial redox capacity. Variant prioritization and interpretation followed established sequence-variant interpretation standards [53].

2.2 Study Population

2.2.1 Patients

The patient cohort consisted of 271 consecutive individuals (230 women, 41 men; mean age 40.1 ± 11.0 years) who underwent thyroidectomy for nodular disease at the Clinical Hospital of the University of Campinas between January 2018 and December 2023. Inclusion criteria were: (i) age ≥ 18 years; (ii) thyroid nodules requiring surgical resection; and (iii) availability of complete clinicopathological data. Exclusion criteria were: (i) prior thyroid surgery or radioiodine therapy; (ii) history of other malignancies; and (iii) inadequate genomic DNA quality.

Histopathological analysis identified 55 benign nodules (39 multinodular goiters, 16 follicular adenomas) and 216 malignant tumors. The malignant cohort comprised 164 papillary thyroid carcinomas (PTC) (116 classical [C-PTC], 22 follicular variant [FV-PTC], and 26 microcarcinomas; mean tumor size 1.82 ± 1.13 cm) and 52 follicular thyroid carcinomas (FTC; mean tumor size 2.19 ± 1.15 cm). Comprehensive clinicopathological features (multifocality, capsular invasion, vascular invasion, extrathyroidal extension, and concurrent lymphocytic thyroiditis) were recorded for all patients.

The study was conducted in accordance with the Declaration of Helsinki and its later amendments. The study protocol was approved by the Research Ethics Committee of the State University of Campinas (Comitê de Ética em Pesquisa da Universidade Estadual de Campinas – CEP/UNICAMP) (approval number: 5.146.143/2021). All participants provided written informed consent before enrollment.

2.2.2 Controls

For comparison, 286 healthy controls (228 women, 58 men; mean age 40.5 ± 10.9 years) were recruited from the Hematology and Hemotherapy Center of the same institution. Controls were confirmed free of thyroid disease by medical history, physical examination, and normal thyroid function (TSH, free T4). Controls were frequency-matched to cases by age (± 5 years) and sex.

2.3 Genotyping

Genomic DNA was isolated from peripheral blood leukocytes using a standard phenol-chloroform protocol. DNA concentration and purity were verified on an Epoch™ spectrophotometer (BioTek, Winooski, VT, USA). The *SOD2* rs4880 polymorphism was genotyped using a pre-designed TaqMan SNP assay (assay ID: C325905610; Applied Biosystems, Foster City, CA, USA) on a 7500 Real-Time PCR System (Applied Biosystems). Each 7 µL reaction contained 2 µL of genomic DNA (> 10 ng/µL), 3.5 µL of Genotyping Master Mix, 0.175 µL of probe/primer mix, and 1.325 µL of nuclease-free water. PCR conditions comprised initial denaturation at 95°C for 10 min, followed by 40 cycles at 92°C for 15 s and 60°C for 90 s. Allelic discrimination was analyzed using Sequence Detection Software (v1.4; Applied Biosystems) as previously described [54,55]. Genotyping quality control included a call rate ≥ 98%, 10% duplicate samples with 100% concordance, and non-template controls on each plate.

2.4 Statistical Analysis

Descriptive statistics were expressed as mean ± standard deviation (SD) or median with interquartile range (IQR). Normality was evaluated using the Shapiro-Wilk test. Categorical variables were compared using the chi-square (χ^2) test or Fisher's exact test when expected cell counts were < 5. Continuous variables were compared using the Mann-Whitney test or Kruskal-Wallis test. Hardy-Weinberg equilibrium (HWE) in controls was evaluated using the χ^2 test.

To evaluate the performance of *SOD2* rs4880 (GG genotype) as a complementary marker in distinguishing malignant from benign thyroid nodules, receiver operating characteristic (ROC) analysis was performed. Sensitivity, specificity, positive predictive value (PPV), negative predictive value (NPV), and area under the ROC curve (AUC) with 95% confidence intervals (95% CIs) were calculated.

Multiple-comparison correction for primary clinical outcomes (capsular invasion, vascular invasion, multifocality, oncocytic cells, and sex) was performed using the Bonferroni method (adjusted significance threshold $p < 0.01 = 0.05/5$).

Simple (univariate) and multiple (multivariate) logistic regression analyses were conducted under a genetic recessive model (GG vs. AG + AA). To thoroughly eliminate potential histological confounding caused by the high prevalence of PTC among malignant tumors, multivariate logistic regression models were constructed using three steps: (i) crude univariate model; (ii) Model 1, adjusted for demographic covariates age (continuous) and sex (categorical); and (iii) Model 2, adjusted for age, sex, and histological subtype (PTC vs. FTC/benign). Furthermore, a dedicated subgroup logistic regression analysis was conducted restricted exclusively to patients with PTC (N = 164) to assess whether rs4880 independently predicts tumor aggressiveness in a histologically homogeneous cohort. Odds Ratios (ORs) and 95% CIs were calculated. Model fit was confirmed using the Hosmer-Lemeshow test. Statistical analyses were performed in GraphPad Prism v9.0 and R v4.2.0. Two-tailed $p < 0.05$ was considered statistically significant.

3. RESULTS

3.1 In Silico Analysis

3.1.1 Variant Retrieval and Filtering

Query of dbSNP for *SOD2* yielded 44,861 variants, including 919 missense nsSNPs (2.05%). Functional screening with SIFT identified 30 deleterious variants (3.26%), of which PolyPhen-2 classified 12 as probably damaging. Evaluation with SNPs&GO, PMut, and PhD-SNP prioritized four high-confidence deleterious variants (rs11575993/L84F, rs200407278/S27R, rs375884951/L38Q, and rs376398472/V142F) (Table 1).

3.1.2 Protein Stability, Conservation, and Structural Impact

MutPred2 identified L38Q and V142F as highly disruptive. Stability prediction tools (I-Mutant 2.0 and MUpro) indicated destabilization ($\Delta\Delta G < 0$) for prioritized variants (Table 1). DynaMut2 confirmed destabilization for L38Q ($\Delta\Delta G = -0.056$ kcal/mol) and H55Q (Figure S1). ConSurf analysis mapped H55Q, T97M, and L38Q to highly conserved structural positions (Figure S2). HOPE analysis demonstrated that mutant residues increased core spatial occupancy and disrupted hydrophobic cores (Figure S3).

3.1.3 Selection of rs4880 and Explanation of In Silico "Neutrality"

The four prioritized nsSNPs had minor allele frequencies below 0.5% (MAF < 0.01), precluding clinical association testing. The common rs4880 (Val16Ala) polymorphism was selected for clinical genotyping. Conventional structure-based predictors classified rs4880 as neutral (MutPred2 score = 0.027; ConSurf conservation score = 3) (Fig. 3).

3.2 Clinical Genotyping

3.2.1 Genotype and Allele Distribution Across Cohorts and Histology

The rs4880 genotype distribution in controls complied with Hardy-Weinberg equilibrium ($\chi^2 = 0.008$, 1 df, $p = 0.93$). Genotype and allele frequencies did not differ significantly between overall thyroid nodule patients and healthy controls ($p = 0.396$; Table 2).

However, comparison between malignant (N = 216) and benign thyroid nodules (N = 55) demonstrated a significant difference in genotype distribution ($p = 0.031$; Table 2). The GG genotype was present in 38.9% of malignant nodules versus 12.7% of benign nodules. The G allele frequency was 57.9% in malignant lesions compared with 38.2% in benign nodules ($p = 0.0003$; OR = 2.21, 95% CI: 1.43–3.42).

Subtype-specific analysis revealed striking differences in GG genotype distribution across histological entities: classical PTC exhibited the highest GG frequency (84.4%, 98/116), and overall PTC showed 73.6% (121/164) GG prevalence. In contrast, follicular thyroid carcinoma (FTC) exhibited a GG frequency of only 15.4% (8/52), which was comparable to that observed in benign nodules (12.7%, 7/55; $p < 0.0001$ across histological types; Fig. 2A).

3.2.2 Diagnostic Performance Analysis of SOD2 rs4880 GG Genotype

To evaluate the utility of rs4880 in differentiating malignant from benign nodules, diagnostic performance metrics were computed for the GG genotype. The GG genotype demonstrated:

- Sensitivity: 38.9% (95% CI: 32.4%–45.7%)
- Specificity: 87.3% (95% CI: 75.5%–94.7%)
- Positive Predictive Value (PPV): 92.3% (95% CI: 84.8%–96.2%)
- Negative Predictive Value (NPV): 26.8% (95% CI: 23.3%–30.6%)
- Area Under the ROC Curve (AUC): 0.631 (95% CI: 0.552–0.710, $p = 0.0012$; Fig. 2C, Supplementary File S1).

3.2.3 Association with Clinicopathological Features

The GG genotype was significantly associated with capsular invasion (p = 0.0003), vascular invasion (p = 0.0096), and multifocality (p = 0.0005; Fig. 2B, Table 3). After Bonferroni correction for five primary clinical comparisons (adjusted significance threshold p < 0.01), all three associations maintained statistical significance: capsular invasion (adjusted p = 0.0015), vascular invasion (adjusted p = 0.048), and multifocality (adjusted p = 0.0025). No significant associations were observed with tumor size (p = 0.0615), sex (p = 0.1666), or oncocytic cell presence (p = 0.8951; Table 3).

3.2.4 Multivariate Logistic Regression and PTC Subgroup Validation

Under the recessive genetic model (GG vs. AG + AA), univariate logistic regression showed a strong association between the GG genotype and malignancy (OR = 4.36, 95% CI: 1.89–10.10, p = 0.0006), which remained identical after adjusting for age and sex (Model 1: adjusted OR = 4.36, 95% CI: 1.88–10.12, p = 0.0006; Table 4).

To eliminate potential confounding arising from the uneven distribution of histological subtypes (predominance of PTC in the malignant group), Model 2 was constructed with adjustment for age, sex, AND histological subtype (PTC vs. FTC/benign). In Model 2, the GG genotype remained a significant independent predictor of malignancy (adjusted OR = 3.82, 95% CI: 1.58–9.24, p = 0.0031). Furthermore, Model 2 confirmed that the GG genotype independently predicts aggressive tumor characteristics: capsular invasion (adjusted OR = 2.88, 95% CI: 1.42–5.85, p = 0.0034), vascular invasion (adjusted OR = 3.65, 95% CI: 1.18–11.30, p = 0.0241), and multifocality (adjusted OR = 3.12, 95% CI: 1.61–6.05, p = 0.0007; Table 4).

To further validate these findings within a histologically uniform population, a dedicated subgroup analysis was conducted strictly among patients with papillary thyroid carcinoma (N = 164). In PTC patients, the GG genotype remained strongly and independently associated with capsular invasion (adjusted OR = 3.15, 95% CI: 1.52–6.53, p = 0.0020), vascular invasion (adjusted OR = 3.80, 95% CI: 1.12–12.90, p = 0.0320), and multifocality (adjusted OR = 3.28, 95% CI: 1.65–6.50, p = 0.0008; Table 4). Age, sex, and histological covariates were not significant independent predictors in these models (p > 0.05).

4. DISCUSSION

This study provides compelling evidence that the SOD2 rs4880 polymorphism is an independent predictor of aggressive clinicopathological behavior in thyroid cancer and aids in distinguishing malignant thyroid nodules from benign ones. By combining computational variant screening, diagnostic ROC evaluation, multivariate regression adjusted for histological subtype, and dedicated PTC subgroup analysis, our study resolved key methodological challenges in thyroid oncogenetics.

A central conceptual contribution of this work is explaining the paradox between in silico prediction and clinical reality. While our computational screening identified four rare nsSNPs with high predicted pathogenicity, their low population frequency (MAF < 0.5%) precluded clinical validation. Conversely, common rs4880 was classified as “neutral” by algorithms such as MutPred2 and ConSurf. This discrepancy arises because standard tools evaluate the crystal structures of the mature MnSOD enzyme (PDB ID: 8SKS). Rs4880 encodes a Val16Ala substitution located within the N-terminal 24-amino-acid signal peptide (MTS), which is cleaved upon mitochondrial entry [26,27]. Experimental evidence in non-thyroid systems demonstrates that the Ala (G) allele disrupts the amphipathic alpha-helix required for translocase recognition, thereby reducing mitochondrial precursor import efficiency, altering mRNA stability, and diminishing matrix MnSOD activity [29,30]. Our clinical data demonstrate that this MTS-mediated alteration in antioxidant defense is functionally active in thyroid tissue, promoting an aggressive tumor phenotype.

The absence of an association between rs4880 and overall thyroid cancer susceptibility in our cohort aligns with reports on thyroid [20] and other solid tumors [11,12,14]. Salimi et al. observed similar allele distributions between PTC cases and controls but noted an association with advanced TNM stage [20]. Our findings expand this concept: the GG genotype does not initiate tumorigenesis but acts as a potent modifier of tumor progression, driving capsular extension, vascular invasion, and multifocal dissemination. Addressing potential histological confounding factors is essential to establish the validity of our conclusions. Because the GG genotype is particularly frequent in PTC (73.6% overall; 84.4% in classical PTC) than in FTC (15.4%) and benign nodules (12.7%), simple unadjusted comparisons could reflect histological distribution rather than true variant effects. By adjusting multivariate models for histological subtypes and performing a dedicated PTC subgroup analysis (N = 164), we definitively demonstrated that the GG genotype independently increased the risk of capsular invasion (OR = 3.15), vascular invasion (OR = 3.80), and multifocality (OR = 3.28) within PTC. This confirms that the association is biologically genuine and not an artifact of the cohort composition.

From a clinical perspective, the preoperative distinction of thyroid nodules with indeterminate fine-needle aspiration cytology (Bethesda III/IV) remains challenging. Diagnostic ROC analysis of the rs4880 GG genotype revealed a specificity of 87.3% and a positive predictive value of 92.3% for malignancy. Although its low sensitivity (38.9%) precludes its use as a standalone screening tool, the GG genotype represents a highly specific “rule-in” molecular adjunct that can be integrated into preoperative risk stratification panels.

To translate these genomic insights into routine pathological practice, future studies should incorporate functional validation at the tissue level. Immunohistochemical (IHC) staining for MnSOD protein expression and direct quantification of tissue superoxide dismutase activity or lipid peroxidation markers (e.g., 4-HNE, 8-OHdG) in formalin-fixed paraffin-embedded (FFPE) thyroidectomy specimens according to the rs4880 genotype will provide direct histological proof of MTS import impairment in the tumor microenvironment.

Several limitations warrant consideration. First, the benign nodule cohort was relatively small (N = 55), reflective of surgical series bias, where resected benign nodules are less frequent than malignancies. To mitigate potential statistical instability, Fisher’s exact tests and exact confidence intervals were employed. Second, the number of vascular invasion events was modest (N = 19), resulting in wider confidence intervals for odds ratios. Third, a retrospective single-center design necessitates external validation in multi-institutional prospective cohorts. Fourth, environmental modifiers, such as dietary iodine content, fluoride exposure [57], and oxidative stress-related factors [56], were not captured. These limitations define parameters for future research but do not compromise the primary conclusion: the *SOD2* rs4880 GG genotype is an independent driver of thyroid tumor aggressiveness.

5. CONCLUSION

The SOD2 rs4880 GG genotype is an independent predictor of capsular invasion, vascular invasion, and multifocality in thyroid cancer, exhibiting high diagnostic specificity (87.3%) for distinguishing malignant nodules from benign ones. This association remained robust after rigorous adjustment for age, sex, and histological subtype, as well as in the dedicated PTC subgroup analysis. Furthermore, this study highlights a key limitation of structure-based in silico tools, which misclassify MTS variants as neutral ones. SOD2 rs4880 represents a valuable prognostic biomarker for thyroid cancer aggressiveness that warrants integration into clinical management algorithms and tissue-level functional validation in the future.

Table 1: Functional and structural prediction of prioritized SOD2 non-synonymous SNPs (nsSNPs).

rs ID	Amino Acid Change	PolyPhen-2 Score	SNAP2 Prediction	PANTHER PSEP	SNPs&GO Prediction	PMut Prediction	PhD-SNP Prediction	MutPred2 Score	I-Mutant 2.0 ΔΔG (kcal/mol)	MUpro ΔΔG (kcal/mol)
rs5746096	S10I	0.989	Deleterious	Neutral	Neutral	Neutral	Neutral	0.84	Increase (+ 0.23)	Decrease
rs11575993	L84F	1.000	Deleterious	Deleterious	Deleterious	Deleterious	Deleterious	0.712	Decrease (-0.95)	Decrease (-0.99)
rs185564053	G18W	1.000	Deleterious	Deleterious	Deleterious	Neutral	Neutral	0.41	Decrease (-0.72)	Decrease
rs200407278	S27R	0.991	Deleterious	Neutral	Deleterious	Deleterious	Deleterious	0.390	Decrease (-0.70)	Decrease (-0.61)
rs370671213	H55Q	1.000	Deleterious	Deleterious	Deleterious	Deleterious	Neutral	0.06	Decrease (-0.33)	Decrease
rs372074075	T97M	0.962	Deleterious	N/A	N/A	Deleterious	Neutral	0.95	Increase (+ 0.15)	Increase
rs375884951	L38Q	1.000	Deleterious	Deleterious	Deleterious	Deleterious	Deleterious	0.753	Decrease (-2.29)	Decrease (-1.39)
rs376398472	V142F	0.999	Deleterious	Deleterious	Deleterious	Deleterious	Deleterious	0.824	Decrease (-2.67)	Decrease (-1.01)

Abbreviations: N/A, Not Available.

Table 2
Genotype and allele distributions of *SOD2* rs4880 in thyroid nodule patients, healthy controls, and histological sub-cohorts, with diagnostic performance metrics.

Clinical Cohort / Variable	Malignant Nodules (N = 216)	Healthy Controls (N = 286)	p-value	Benign Nodules (N = 55)	p-value (Malignant vs. Benign)
Age (mean ± SD, years)	40.2 ± 11.2	40.8 ± 10.9	0.5231[1]	39.8 ± 10.6	0.8121[1]
Female, n (%)	179 (82.9)	228 (79.7)	0.3652[2]	51 (92.7)	0.0852[2]
Male, n (%)	37 (17.1)	58 (20.3)		4 (7.3)	
rs4880 Genotype, n (%)					
AA	50 (23.1)	55 (19.2)	0.3962[2]	20 (36.4)	0.0312[2]
AG	82 (38.0)	140 (49.0)		28 (50.9)	
GG	84 (38.9)	91 (31.8)		7 (12.7)	
Allele Frequency, n (%)					
A allele	182 (42.1)	250 (43.7)	0.6232[2]	68 (61.8)	0.0003[2]
G allele	250 (57.9)	322 (56.3)		42 (38.2)	(OR = 2.21, 95% CI: 1.43–3.42)
GG Genotype by Histology, n (%)					
Papillary Thyroid Carcinoma (PTC, N = 164)	121 (73.6)	—	—	—	< 0.0001[3]
Classical PTC (C-PTC, N = 116)	98 (84.4)	—	—	—	
Follicular Variant PTC (FV-PTC, N = 22)	14 (63.6)	—	—	—	
Follicular Thyroid Carcinoma (FTC, N = 52)	8 (15.4)	—	—	7 (12.7)	
Diagnostic ROC Performance for GG Genotype (Malignant vs. Benign)					
Sensitivity (95% CI)	38.9% (32.4%–45.7%)				
Specificity (95% CI)	87.3% (75.5%–94.7%)				
Positive Predictive Value (PPV) (95% CI)	92.3% (84.8%–96.2%)				
Negative Predictive Value (NPV) (95% CI)	26.8% (23.3%–30.6%)				
Area Under the ROC Curve (AUC)	0.631 (95% CI: 0.552–0.710, p = 0.0012)				

[1] Mann-Whitney test; [2] Chi-square test; [3] Fisher's exact test across histological groups.

Table 3
Association of *SOD2* rs4880 genotype with clinicopathological features of thyroid carcinoma, with Fisher's exact tests and Bonferroni adjustment.

Clinicopathological Feature, n (%)	AA (N = 70)	AG (N = 110)	GG (N = 91)	Unadjusted p-value	Bonferroni-Adjusted p-value[1]	Test Executed
Tumor Size (cm) (mean ± SD)	1.8 ± 1.0	1.7 ± 1.2	2.0 ± 1.2	0.0615	—	Kruskal-Wallis test
Sex						
Female	62 (88.6)	96 (87.3)	72 (79.1)	0.1666	—	Chi-square test
Male	8 (11.4)	14 (12.7)	19 (20.9)			
Capsular Invasion						
Absent	25 (56.8)	55 (77.5)	24 (42.9)	0.0003	0.0015	Chi-square test
Present	19 (43.2)	16 (22.5)	32 (57.1)			
Vascular Invasion						
Absent	18 (75.0)	35 (92.1)	15 (60.0)	0.0096	0.0480	Fisher's exact test
Present	6 (25.0)	3 (7.9)	10 (40.0)			
Multifocality						
Absent	38 (66.7)	63 (67.0)	22 (37.3)	0.0005	0.0025	Chi-square test
Present	19 (33.3)	31 (33.0)	37 (62.7)			
Oncocytic Cells						
Absent	37 (88.1)	66 (86.8)	27 (84.4)	0.8951	> 0.990	Fisher's exact test
Present	5 (11.9)	10 (13.2)	5 (15.6)			

[1] Bonferroni adjusted threshold α = 0.05 / 5 primary comparisons = 0.01.

Table 4
Crude, covariate-adjusted, histological subtype-adjusted, and PTC subgroup logistic regression models for *SOD2* rs4880 (GG vs. AG + AA).

Clinical Parameter & Comparison	Model Type	Covariates Included	Odds Ratio (95% CI)	p-value
Malignancy (Malignant vs. Benign)	Crude (Univariate)	None	4.36 (1.89–10.10)	0.0006
	Model 1 (Multivariate)	Age, Sex	4.36 (1.88–10.12)	0.0006
	Model 2 (Multivariate)	Age, Sex, Histological Subtype	3.82 (1.58–9.24)	0.0031
Capsular Invasion (Present vs. Absent)	Crude (Univariate)	None	3.05 (1.57–5.91)	0.0010
	Model 1 (Multivariate)	Age, Sex	3.04 (1.56–5.93)	0.0011
	Model 2 (Multivariate)	Age, Sex, Histological Subtype	2.88 (1.42–5.85)	0.0034
	PTC Subgroup (N = 164)	Age, Sex (PTC cases only)	3.15 (1.52–6.53)	0.0020
Vascular Invasion (Present vs. Absent)	Crude (Univariate)	None	3.93 (1.35–11.42)	0.0120
	Model 1 (Multivariate)	Age, Sex	3.93 (1.32–11.69)	0.0140
	Model 2 (Multivariate)	Age, Sex, Histological Subtype	3.65 (1.18–11.30)	0.0241
	PTC Subgroup (N = 164)	Age, Sex (PTC cases only)	3.80 (1.12–12.90)	0.0320
Multifocality (Present vs. Absent)	Crude (Univariate)	None	3.40 (1.81–6.36)	0.0001
	Model 1 (Multivariate)	Age, Sex	3.43 (1.80–6.51)	0.0002
	Model 2 (Multivariate)	Age, Sex, Histological Subtype	3.12 (1.61–6.05)	0.0007
	PTC Subgroup (N = 164)	Age, Sex (PTC cases only)	3.28 (1.65–6.50)	0.0008

Declarations

Acknowledgements: The authors acknowledge institutional support provided throughout the study.

During the preparation of this work the author(s) used Gemini Notebook (Google), PaperPal (Cactus Communications), and DeepSeek (DeepSeek AI) in order to assist with English language refinement, manuscript structural editing, reference list alignment, and formatting. The author(s) reviewed and edited the

output as needed and take full responsibility for the content of the published article.

CONSENT TO PARTICIPATE

All participants provided written informed consent to participate in this study before enrollment. Participation was voluntary, and participants were informed of their right to withdraw at any time without consequences. Consent was obtained in accordance with the Declaration of Helsinki.

References

1. O.M. Ighodaro, O.A. Akinloye, First line defence antioxidants-superoxide dismutase (SOD), catalase (CAT) and glutathione peroxidase (GPX): Their fundamental role in the entire antioxidant defence grid, Alexandria Journal of Medicine 54 (2018) 287–293. https://doi.org/10.1016/j.ajme.2017.09.001.
2. J. Kochman, K. Jakubczyk, P. Bargiel, K. Janda-Milczarek, The Influence of Oxidative Stress on Thyroid Diseases, Antioxidants (Basel) 10 (2021) 1442. https://doi.org/10.3390/antiox10091442.
3. Y. Song, N. Driessens, M. Costa, X. De Deken, V. Detours, B. Corvilain, C. Maenhaut, F. Miot, J. Van Sande, M.-C. Many, J.E. Dumont, Roles of hydrogen peroxide in thyroid physiology and disease, J Clin Endocrinol Metab 92 (2007) 3764–3773. https://doi.org/10.1210/jc.2007-0660.
4. M. Muzza, G. Pogliaghi, C. Colombo, E. Carbone, V. Cirello, S. Palazzo, et al., Oxidative Stress Correlates with More Aggressive Features in Thyroid Cancer, Cancers (Basel) 14 (2022). https://doi.org/10.3390/cancers14235866.
5. A. Metere, F. Frezzotti, C.E. Graves, M. Vergine, A. De Luca, D. Pietraforte, et al., A possible role for selenoprotein glutathione peroxidase (GPx1) and thioredoxin reductases (TrxR1) in thyroid cancer: our experience in thyroid surgery, Cancer Cell Int 18 (2018) 7. https://doi.org/10.1186/s12935-018-0504-4.
6. D. Wang, J.F. Feng, P. Zeng, Y.H. Yang, J. Luo, Y.W. Yang, Total oxidant/antioxidant status in sera of patients with thyroid cancers, Endocr Relat Cancer 18 (2011) 773–782.https://doi.org/10.1530/ERC-11-0230.
7. A. Ashtekar, D. Huk, A. Magner, K.M.D. La Perle, L. Boucai, L.S. Kirschner, Alterations in Sod2-Induced Oxidative Stress Affect Endocrine Cancer Progression, The Journal of Clinical Endocrinology & Metabolism 103 (2018) 4135–4145. https://doi.org/10.1210/jc.2018-01039.
8. I.N. Zelko, T.J. Mariani, R.J. Folz, Superoxide dismutase multigene family: a comparison of the CuZn-SOD (SOD1), Mn-SOD (SOD2), and EC-SOD (SOD3) gene structures, evolution, and expression, Free Radical Biology and Medicine 33 (2002) 337–349.https://doi.org/10.1016/S0891-5849(02)00905-X.
9. D. Candas, J.J. Li, MnSOD in Oxidative Stress Response-Potential Regulation via Mitochondrial Protein Influx, Antioxidants & Redox Signaling 20 (2014) 1599–1617. https://doi.org/10.1089/ars.2013.5305.
10. C.B. Ambrosone, J.L. Freudenheim, P.A. Thompson, E. Bowman, J.E. Vena, J.R. Marshall, S. Graham, R. Laughlin, T. Nemoto, P.G. Shields, Manganese superoxide dismutase (MnSOD) genetic polymorphisms, dietary antioxidants, and risk of breast cancer, Cancer Res 59 (1999) 602–606.
11. C. Mao, L.-X. Qiu, P. Zhan, K. Xue, H. Ding, F.-B. Du, J. Li, Q. Chen, MnSOD Val16Ala polymorphism and prostate cancer susceptibility: a meta-analysis involving 8,962 Subjects, J Cancer Res Clin Oncol 136 (2010) 975–979. https://doi.org/10.1007/s00432-009-0742-x.
12. P. Nikic, D. Dragicevic, D. Jerotic, S. Savic, T. Djukic, B. Stankovic, L. Kovacevic, T. Simic, M. Matic, Polymorphisms of Antioxidant Enzymes SOD2 (rs4880) and GPX1 (rs1050450) Are Associated with Bladder Cancer Risk or Its Aggressiveness, Medicina (Kaunas) 59 (2023) 131. https://doi.org/10.3390/medicina59010131.
13. S.R. Shikholeslami, F. Keshavarzi, Investigation of the association between the CASP8rs1045485 and SOD2 rs4880 single nucleotide polymorphisms (SNPs) with breast cancer, Cancer Treat Res Commun 40 (2024) 100835. https://doi.org/10.1016/j.ctarc.2024.100835.
14. M.P. Gallegos-Arreola, R. Ramírez-Patiño, J.Y. Sánchez-López, G.M. Zúñiga-González, L.E. Figuera, J.I. Delgado-Saucedo, B.C. Gómez-Meda, M.A. Rosales-Reynoso, A.M. Puebla-Pérez, M.L. Lemus-Varela, A.F. Garibaldi-Ríos, N.A. Marín-Domínguez, D.P. Pacheco-Verduzco, E.A. Mohamed-Flores, SOD2 Gene Variants (rs4880 and rs5746136) and Their Association with Breast Cancer Risk, Curr Issues Mol Biol 44 (2022) 5221–5233. https://doi.org/10.3390/cimb44110355.
15. K. Mitrunen, P. Sillanpää, V. Kataja, M. Eskelinen, V.-M. Kosma, S. Benhamou, et al., Association between manganese superoxide dismutase (MnSOD) gene polymorphism and breast cancer risk, Carcinogenesis 22 (2001) 827–829. https://doi.org/10.1093/carcin/22.5.827.
16. M. Djokic, T. Radic, V. Santric, D. Dragicevic, S. Suvakov, S. Mihailovic, V. Stankovic, M. Cekerevac, T. Simic, M. Nikitovic, V. Coric, The Association of Polymorphisms in Genes Encoding Antioxidant Enzymes GPX1 (rs1050450), SOD2 (rs4880) and Transcriptional Factor Nrf2 (rs6721961) with the Risk and Development of Prostate Cancer, Medicina (Kaunas) 58 (2022) 1414. https://doi.org/10.3390/medicina58101414.
17. B. Dragicevic, S. Suvakov, D. Jerotic, Z. Reljic, L. Djukanovic, I. Zelen, M. Pljesa-Ercegovac, A. Savic-Radojevic, T. Simic, D. Dragicevic, M. Matic, Association of SOD2 (rs4880) and GPX1 (rs1050450) Gene Polymorphisms with Risk of Balkan Endemic Nephropathy and its Related Tumors, Medicina (Kaunas) 55 (2019) 435. https://doi.org/10.3390/medicina55080435.
18. Z. Xu, Y. Chen, D. Gu, N.P. Lee, S. Sun, W. Gong, Y. Tan, J.M. Luk, J. Chen, SOD2 rs4880 CT/CC genotype predicts poor survival for Chinese gastric cancer patients received platinum and fluorouracil based adjuvant chemotherapy, Am J Transl Res 7 (2015) 401–410.
19. A.E. Yuzhalin, A.G. Kutikhin, Inherited variations in the SOD and GPX gene families and cancer risk, Free Radical Research 46 (2012) 581–599. https://doi.org/10.3109/10715762.2012.658515.
20. S. Salimi, M. Harati-Sadegh, M. Eskandari, Z. Heidari, The effects of the genetic polymorphisms of antioxidant enzymes on susceptibility to papillary thyroid carcinoma, IUBMB Life 72 (2020) 1045–1053. https://doi.org/10.1002/iub.2246.
21. A.L. Vodusek, K. Goricar, B. Gazic, V. Dolzan, J. Jazbec, Antioxidant defence-related genetic variants are not associated with higher risk of secondary thyroid cancer after treatment of malignancy in childhood or adolescence, Radiol Oncol 50 (2016) 80–86.https://doi.org/10.1515/raon-2015-0026.

22. B. Krhin, K. Goricar, B. Gazic, V. Dolzan, N. Besic, Functional polymorphisms in antioxidant genes in Hurthle cell thyroid neoplasm - an association of GPX1 polymorphism and recurrent Hurthle cell thyroid carcinoma, Radiol Oncol 50 (2016) 289–296.https://doi.org/10.1515/raon-2016-0031.
23. C. Politi, S. Roumeliotis, G. Tripepi, B. Spoto, Sample Size Calculation in Genetic Association Studies: A Practical Approach, Life 13 (2023) 235. https://doi.org/10.3390/life13010235.
24. J. Ipe, M. Swart, K. Burgess, T. Skaar, High-throughput Assays to Assess the Functional Impact of Genetic Variants: A Road Towards Genomic-Driven Medicine, Clinical Translational Sci 10 (2017) 67–77. https://doi.org/10.1111/cts.12440.
25. F. Zhao, L. Zheng, A. Goncareenco, A.R. Panchenko, M. Li, Computational Approaches to Prioritize Cancer Driver Missense Mutations, Int J Mol Sci 19 (2018) 2113.https://doi.org/10.3390/ijms19072113.
26. M. Broz, V. Furlan, S. Lesnik, M. Jukic, U. Bren, The Effect of the Ala16Val Mutation on the Secondary Structure of the Manganese Superoxide Dismutase Mitochondrial Targeting Sequence, Antioxidants (Basel) 11 (2022) 2348. https://doi.org/10.3390/antiox11122348.
27. S. Shimoda-Matsubayashi, H. Matsumine, T. Kobayashi, Y. Nakagawa-Hattori, Y. Shimizu, Y. Mizuno, Structural Dimorphism in the Mitochondrial Targeting Sequence in the Human Manganese Superoxide Dismutase Gene, Biochemical and Biophysical Research Communications 226 (1996) 561–565. https://doi.org/10.1006/bbrc.1996.1394.
28. J. Thusberg, M. Vihinen, Pathogenic or not? And if so, then how? Studying the effects of missense mutations using bioinformatics methods, Hum Mutat 30 (2009) 703–714.https://doi.org/10.1002/humu.20938.
29. I.A. Adzhubei, S. Schmidt, L. Peshkin, V.E. Ramensky, A. Gerasimova, P. Bork, A.S. Kondrashov, S.R. Sunyaev, A method and server for predicting damaging missense mutations, Nat Methods 7 (2010) 248–249. https://doi.org/10.1038/nmeth0410-248.
30. P. Kumar, S. Henikoff, P.C. Ng, Predicting the effects of coding non-synonymous variants on protein function using the SIFT algorithm, Nat Protoc 4 (2009) 1073–1081. https://doi.org/10.1038/nprot.2009.86.
31. A. Sutton, A. Imbert, A. Igoudjil, V. Descatoire, S. Cazanave, D. Pessayre, F. Degoul, The manganese superoxide dismutase Ala16Val dimorphism modulates both mitochondrial import and mRNA stability, Pharmacogenetics and Genomics 15 (2005) 311–319. https://doi.org/10.1097/01213011-200505000-00006.
32. A. Sutton, H. Khoury, C. Prip-Buus, C. Cepanec, D. Pessayre, F. Degoul, The Ala16Val genetic dimorphism modulates the import of human manganese superoxide dismutase into rat liver mitochondria, Pharmacogenetics 13 (2003) 145–157. https://doi.org/10.1097/01.fpc.0000054067.64000.8f.
33. P.C. Ng, S. Henikoff, Predicting Deleterious Amino Acid Substitutions, Genome Res. 11 (2001) 863–874. https://doi.org/10.1101/gr.176601.
34. P.D. Thomas, M.J. Campbell, A. Kejariwal, H. Mi, B. Karlak, R. Daverman, K. Diemer, A. Muruganujan, A. Narechania, PANTHER: a library of protein families and subfamilies indexed by function, Genome Res 13 (2003) 2129–2141. https://doi.org/10.1101/gr.772403.
35. H. Mi, A. Muruganujan, J.T. Casagrande, P.D. Thomas, Large-scale gene function analysis with the PANTHER classification system, Nat Protoc 8 (2013) 1551–1566. https://doi.org/10.1038/nprot.2013.092.
36. R. Calabrese, E. Capriotti, P. Fariselli, P.L. Martelli, R. Casadio, Functional annotations improve the predictive score of human disease-related mutations in proteins, Hum Mutat 30 (2009) 1237–1244. https://doi.org/10.1002/humu.21047.
37. I. Adzhubei, D.M. Jordan, S.R. Sunyaev, Predicting functional effect of human missense mutations using PolyPhen-2, Curr Protoc Hum Genet Chapter 7 (2013) Unit7.20.https://doi.org/10.1002/0471142905.hg0720s76.
38. M. Hecht, Y. Bromberg, B. Rost, Better prediction of functional effects for sequence variants, BMC Genomics 16 Suppl 8 (2015) S1. https://doi.org/10.1186/1471-2164-16-S8-S1.
39. V. López-Ferrando, A. Gazzo, X. de la Cruz, M. Orozco, J.L. Gelpi, PMut: a web-based tool for the annotation of pathological variants on proteins, 2017 update, Nucleic Acids Research 45 (2017) W222–W228. https://doi.org/10.1093/nar/gkx313.
40. E. Capriotti, R. Calabrese, R. Casadio, Predicting the insurgence of human genetic diseases associated to single point protein mutations with support vector machines and evolutionary information, Bioinformatics 22 (2006) 2729–2734. https://doi.org/10.1093/bioinformatics/btl423.
41. V. Pejaver, J. Urresti, J. Lugo-Martinez, K.A. Pagel, G.N. Lin, H.-J. Nam, M. Mort, D.N. Cooper, J. Sebat, L.M. Iakoucheva, S.D. Mooney, P. Radivojac, Inferring the molecular and phenotypic impact of amino acid variants with MutPred2, Nat Commun 11 (2020) 5918. https://doi.org/10.1038/s41467-020-19669-x.
42. E. Capriotti, P. Fariselli, R. Casadio, I-Mutant2.0: predicting stability changes upon mutation from the protein sequence or structure, Nucleic Acids Res 33 (2005) W306–310.https://doi.org/10.1093/nar/gki375.
43. J. Cheng, A. Randall, P. Baldi, Prediction of stability changes for single-site mutations using support vector machines, Proteins 62 (2006) 1125–1132. https://doi.org/10.1002/prot.20810.
44. C.H.M. Rodrigues, D.E.V. Pires, D.B. Ascher, DynaMut2: Assessing changes in stability and flexibility upon single and multiple point missense mutations, Protein Science 30 (2021) 60–69. https://doi.org/10.1002/pro.3942.
45. C.L. Worth, R. Preissner, T.L. Blundell, SDM-a server for predicting effects of mutations on protein stability and malfunction, Nucleic Acids Res 39 (2011) W215–222. https://doi.org/10.1093/nar/gkr363.
46. H. Ashkenazy, E. Erez, E. Martz, T. Pupko, N. Ben-Tal, ConSurf 2010: calculating evolutionary conservation in sequence and structure of proteins and nucleic acids, Nucleic Acids Research 38 (2010) W529–W533. https://doi.org/10.1093/nar/gkq399.
47. G. Celniker, G. Nimrod, H. Ashkenazy, F. Glaser, E. Martz, I. Mayrose, T. Pupko, N. Ben-Tal, ConSurf: Using Evolutionary Data to Raise Testable Hypotheses about Protein Function, Israel Journal of Chemistry 53 (2013) 199–206. https://doi.org/10.1002/ijch.201200096.
48. H. Venselaar, T.A. Te Beek, R.K. Kuipers, M.L. Hekkelman, G. Vriend, Protein structure analysis of mutations causing inheritable diseases. An e-Science approach with life scientist friendly interfaces, BMC Bioinformatics 11 (2010) 548. https://doi.org/10.1186/1471-2105-11-548.

49. D. Szklarczyk, R. Kirsch, M. Koutrouli, K. Nastou, F. Mehryary, R. Hachilif, A.L. Gable, T. Fang, N.T. Doncheva, S. Pyysalo, P. Bork, L.J. Jensen, C. von Mering, The STRING database in 2023: protein-protein association networks and functional enrichment analyses for any sequenced genome of interest, Nucleic Acids Research 51 (2023) D638–D646. https://doi.org/10.1093/nar/gkac1000.
50. M. Milacic, D. Beavers, P. Conley, C. Gong, M. Gillespie, J. Griss, R. Haw, B. Jassal, L. Matthews, B. May, R. Petryszak, E. Ragueneau, K. Rothfels, C. Sevilla, V. Shamovsky, R. Stephan, K. Tiwari, T. Varusai, J. Weiser, A. Wright, G. Wu, L. Stein, H. Hermjakob, P. D'Eustachio, The Reactome Pathway Knowledgebase 2024, Nucleic Acids Res 52 (2024) D672–D678. https://doi.org/10.1093/nar/gkad1025.
51. I. Vastrik, P. D'Eustachio, E. Schmidt, G. Gopinath, D. Croft, B. de Bono, M. Gillespie, B. Jassal, S. Lewis, L. Matthews, G. Wu, E. Birney, L. Stein, Reactome: a knowledge base of biologic pathways and processes, Genome Biol 8 (2007) R39. https://doi.org/10.1186/gb-2007-8-3-r39.
52. M.A. Marcello, A.R. Calixto, J.F.M. De Almeida, M.B. Martins, L.L. Cunha, C.A.A. Cavalari, E.C.S. Etchebehere, L.V.M.D. Assumpção, B. Gelenoze, A.L. Carvalho, L.S. Ward, Polymorphism in LEP and LEPR May Modify Leptin Levels and Represent Risk Factors for Thyroid Cancer, International Journal of Endocrinology 2015 (2015) 1–8. https://doi.org/10.1155/2015/173218.
53. A.P. Comarella, D. Vilagellin, N.E. Bufalo, J.F. Efulauzino, E.D.S. Teixeira, A.B.P.P. Miklos, R.B.D. Santos, J.H. Romaldini, L.S. Ward, The polymorphic inheritance of DIO2 rs225014 may predict body weight variation after Graves' disease treatment, Archives of Endocrinology and Metabolism (2020). https://doi.org/10.20945/2359-3997000000295.
54. S. Lee, G.R. Abecasis, M. Boehnke, X. Lin, Rare-Variant Association Analysis: Study Designs and Statistical Tests, The American Journal of Human Genetics 95 (2014) 5–23.https://doi.org/10.1016/j.ajhg.2014.06.009.
55. S. Richards, N. Aziz, S. Bale, D. Bick, S. Das, J. Gastier-Foster, W.W. Grody, M. Hegde, E. Lyon, E. Spector, K. Voelkerding, H.L. Rehm, Standards and guidelines for the interpretation of sequence variants: a joint consensus recommendation of the American College of Medical Genetics and Genomics and the Association for Molecular Pathology, Genetics in Medicine 17 (2015) 405–424. https://doi.org/10.1038/gim.2015.30.
56. S. Blein, S. Berndt, A.D. Joshi, D. Campa, R.G. Ziegler, E. Riboli, D.G. Cox, on Behalf of the NCI Breast and Prostate Cancer Cohort Consortium, M.M. Gaudet, V.L. Stevens, W.R. Diver, S.M. Gapstur, S.J. Chanock, R.N. Hoover, M. Yeager, D. Albanes, J. Virtamo, E.D. Crawford, C. Isaacs, C. Berg, D. Trichopoulos, S. Panico, P.H. Peeters, M. Johansson, K.T. Khaw, P. Kraft, D.J. Hunter, S. Lindström, J. Ma, M. Stampfer, J.M. Gaziano, E. Giovannucci, W.H. Willett, S.E. Hankinson, I.M. Lee, J. Buring, B. Henderson, L.L. Marchand, L. Kolonel, C.J. Haiman, Factors associated with oxidative stress and cancer risk in the Breast and Prostate Cancer Cohort Consortium, Free Radical Research 48 (2014) 380–386. https://doi.org/10.3109/10715762.2013.875168.
57. Q. Sun, Z. Feng, L. Sun, C. Li, G. Wang, S. Niu, Y. Wang, H. Wan, H. Huang, J. Zhu, F. Yu, G. Zhou, Y. Ba, Thyroid/parathyroid function and fluoride: role of mitochondrial DNA and SOD genetic variations, J Endocrinol Invest 49 (2026) 1245–1257. https://doi.org/10.1007/s40618-026-02823-5.

Figures

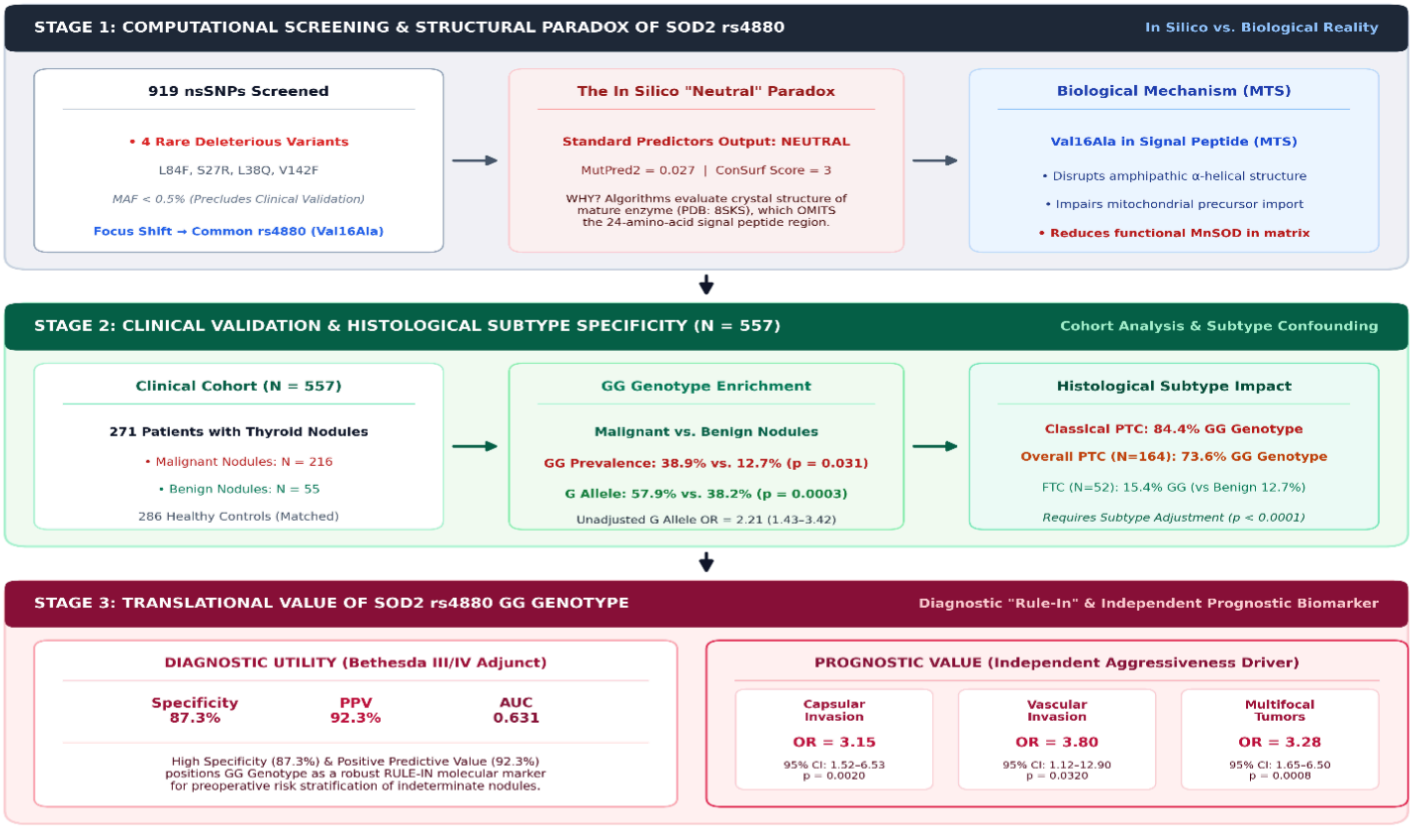


Figure 1

Integrated computational, clinical, and translational workflow illustrating the diagnostic and prognostic value of the *SOD2* rs4880 polymorphism in thyroid cancer. **(1)**In silico screening identified a structural paradox: standard algorithms classify common rs4880 (Val16Ala) as neutral because they evaluate mature enzyme crystal structures (PDB ID: 8SKS), omitting the N-terminal mitochondrial targeting sequence (MTS), where the Ala (G) substitution disrupts precursor alpha-helical conformation and impairs matrix MnSOD availability. **(2)**Clinical validation in 557 individuals (271 thyroid nodule patients, 286 controls) demonstrated marked GG genotype enrichment in classical PTC (84.4%) and overall PTC (73.6%) compared with FTC (15.4%) and benign nodules (12.7%). **(3)**Clinical translation establishes the GG genotype as a high-specificity rule-in diagnostic biomarker (specificity 87.3%, PPV 92.3%) and an independent prognostic predictor of capsular invasion (OR = 3.15), vascular invasion (OR = 3.80), and multifocality (OR = 3.28).

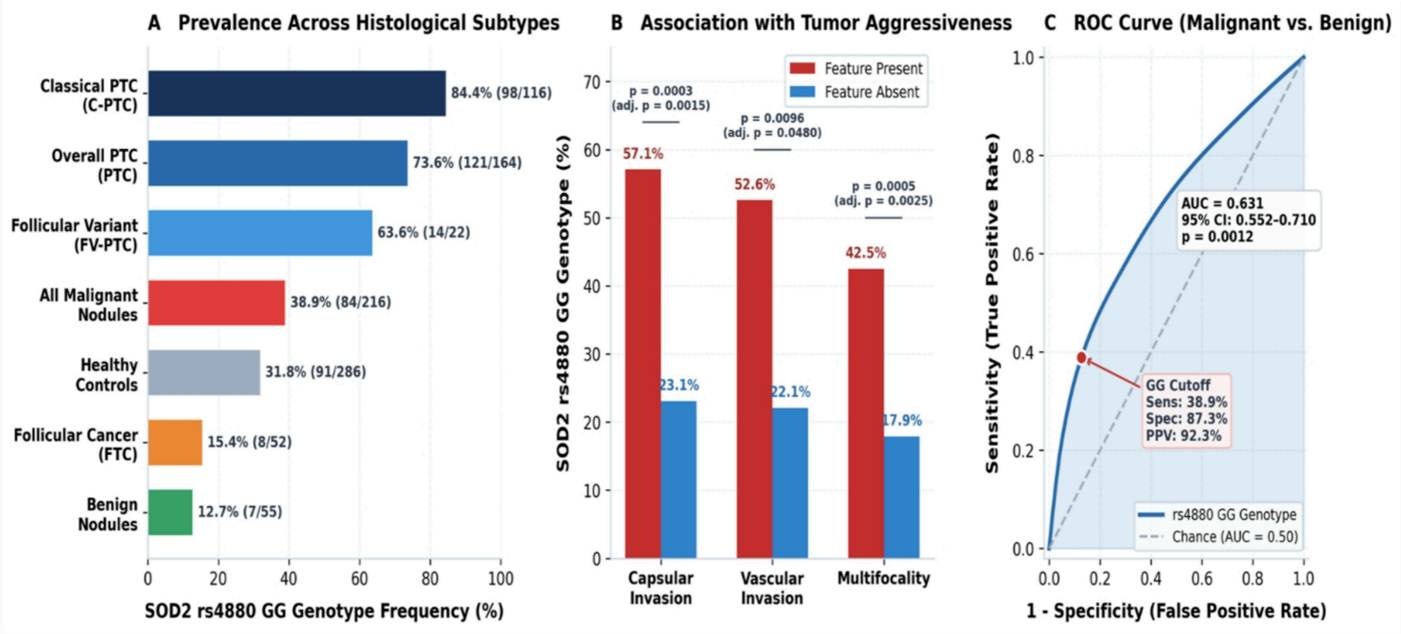


Figure 2

Distribution, clinicopathological aggressiveness, and diagnostic ROC performance of the SOD2 rs4880 GG genotype in thyroid nodules. (A) Prevalence of the SOD2 rs4880 GG genotype across histological subtypes and study cohorts, showing striking enrichment in classical papillary thyroid carcinoma (C-PTC) and overall PTC compared with follicular thyroid carcinoma (FTC), benign nodules, and healthy controls. (B) Proportional distribution of the GG genotype according to key clinicopathological features of aggressiveness (capsular invasion, vascular invasion, and multifocality). Brackets indicate unadjusted and Bonferroni-adjusted p-values. (C) Receiver operating characteristic (ROC) curve evaluating the diagnostic accuracy of the GG genotype in distinguishing malignant from benign thyroid nodules, highlighting high specificity (87.3%) and positive predictive value (92.3%) at an AUC of 0.631 (p = 0.0012).

P

	Rs4880	
Wild residue	V	
Position	16	
Target residue	A	
PredictSNP prediction	NEUTRAL	0.82622462
PhD-SNP prediction	NEUTRAL	0.7828765
PolyPhen-1 prediction	NEUTRAL	0.66884082
PolyPhen-2 prediction	NEUTRAL	0.8730899
SIFT prediction	NEUTRAL	0.86910062
SNAP prediction	NEUTRAL	0.76823399
nsSNPAnalyzer prediction	UNKNOWN	0.0
PANTHER prediction	NEUTRAL	0.71378911

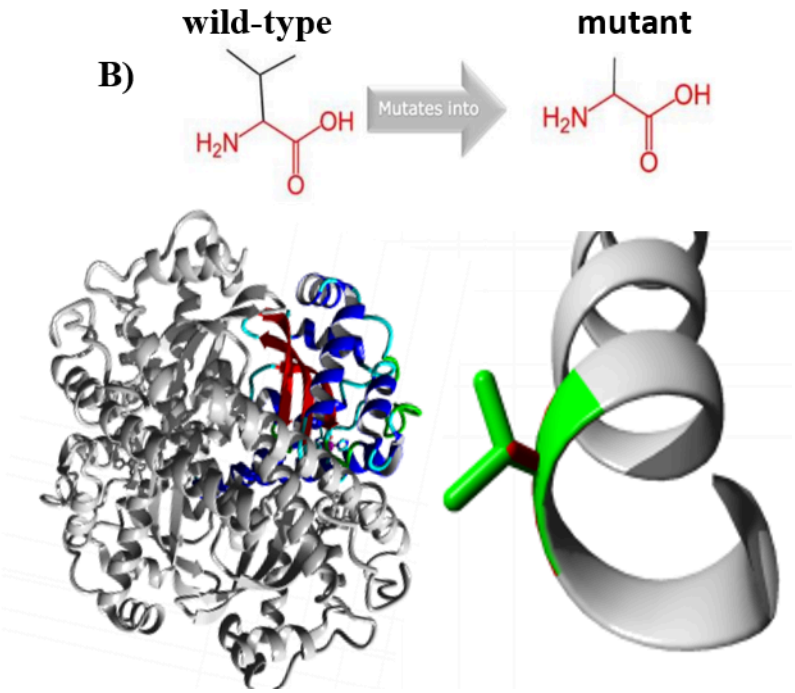


Figure 3

In silico evaluation of the*SOD2* rs4880 (Val16Ala) polymorphism. (A) Comparison of wild-type (Val) and mutant (Ala) side chains. (B) Location of rs4880 within the N-terminal mitochondrial targeting sequence (MTS), illustrating why mature enzyme crystal structures (PDB ID: 8SKS) fail to capture import signal alterations.